Sensors and Materials, Vol. 37, No. 3 (2025) 1229–1242
MYU Tokyo

S & M 3983

Applying Wavelet Transform to Detection of Encoder Failures in Train Door Motors

Chien-Chi Chiu,[1] Ming-Tsung Yeh,[2*] Chun-Yu Liu,[3] and Yi-Nung Chung[1]

[1]Department of Electrical Engineering, National Changhua University of Education,
No. 1, Jinde Rd., Changhua City, Changhua County 50007, Taiwan
[2]Department of Electrical Engineering, National Chin-Yi University of Technology,
57, Sec. 2, Zhongshan Rd., Taiping Dist, Taichung 411030, Taiwan
[3]Railway System Division, Mechanical and Mechatronics Systems Research Labs,
Industrial Technology Research Institute,
195, Sec. 4, Chung Hsing Rd., Chutung, Hsinchu 310401, Taiwan

(Received June 29, 2024; accepted March 14, 2025)

Keywords: railway train, door control system, wavelet transform, motor encoder, fault detection

Railway trains represent a vital component of transportation infrastructure in numerous countries. Railway travel offers individuals convenient and secure transportation options. The paramount concern for the general public is the safety of railway trains, particularly the dependability and security of the door control system. The motor encoder is essential, and in the event of a malfunction, it has the potential to result in abnormal door operation, which could lead to significant safety risks. To prevent potential malfunctions, the door control system must be designed to detect any anomalous noise and promptly halt operation. In the event of encoder detachment or poor contact with the encoder wire, which is a common occurrence, the system must be capable of detecting such anomalies with immediate effect. In this study, a multiscale wavelet transform is proposed to transform the velocity data of the motor encoder. The resulting curve identifies and accentuates the distinctive attributes of anomalous signals, thereby facilitating the expeditious detection of encoder malfunctions in the door control system. The wavelet transform converts the standard encoder velocity signals for learning and analysis. Following this, any noise caused by encoder detachment or poor contact with the encoder wire is identified. Subsequently, the controller utilizes the distinctive characteristics of anomalous encoder signals to guarantee the prompt cessation of door operation in case of a motor encoder failure. Verification has demonstrated that this method not only rapidly converts and highlights abnormal encoder signals but also effectively ensures the safe operation of the railway train door system.

1. Introduction

While ensuring safety, many studies on train control systems focus on the strategies for controlling the opening and closing of train and platform doors.[1–3] Systems for both operations

*Corresponding author: e-mail: mtyeh@ncut.edu.tw
https://doi.org/10.18494/SAM5223

ISSN 0914-4935
https://myukk.org/

require motor power to drive and pull the doors, making motor fault detection crucial in railway systems.[4–6] EN 61800-5-3 is a standard developed by the International Electrotechnical Commission that specifies safety performance criteria for variable-frequency drives. This standard pertains to adjustable-speed electric drive systems powered by electric motors, including control systems, power electronic devices, and motors. It delineates the fundamental requirements for designing and constructing variable-frequency drives, including electrical, mechanical, and functional considerations, as well as specifications for motor encoders. The standard provides verification methods and evaluation procedures to ensure compliance, including testing, simulation, and analysis.

Integrating sensors into railway door control systems enhances monitoring capabilities, allowing for the real-time detection of anomalies. There are numerous methodologies and techniques for analyzing motor and encoder malfunctions. One such technique is the utilization of machine learning for the diagnosis of faults in electric drives. However, machine learning models are not without limitations. They are typically constrained to diagnosing faults for which they have been trained and can be costly to implement on computational platforms.[7] Furthermore, using motor current for fault detection can be challenging because of the coupling of motor current signals with noise, making it difficult to accurately detect faults and effectively diagnose encoder failures.[8]

As illustrated in Fig. 1, this study employs a wavelet transform method integrated with encoder data to derive a motor speed curve that is both reasonable and accurate. The technique is both simple and efficient in its computation, and it offers superior identification and more responsive detection than existing signal detection methods.

In general, motor current signals frequently contain a considerable amount of noise, which presents a significant challenge to accurately detecting errors. To address this issue, a signal filtering process must be implemented. Although Fourier transform methods can detect motor current signals by converting them into different frequency components,[9–13] they cannot provide real-time frequency information as it changes over time. In contrast, the wavelet transform is an effective solution to this limitation. The

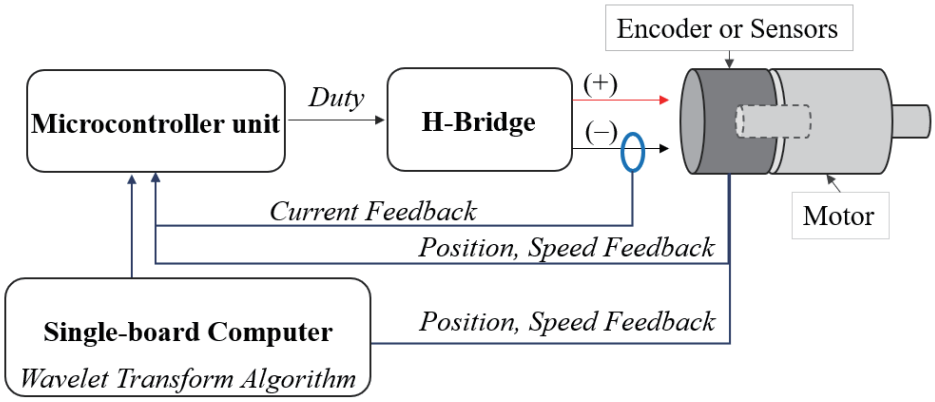

Fig. 1. (Color online) Architectural diagram of wavelet transform of encoder data applied to the motor fault detection system.

original signal is decomposed into variable-time and -frequency windows, facilitating a more effective capture of signal changes. Wavelet transform employs two distinct methodologies: Continuous wavelet transform (CWT) and discrete wavelet transform (DWT).[14–17] In this study, we employ the DWT, which is typically utilized for processing signals within a specified range.

The wavelet transform is a widely utilized signal processing technique that can effectively decompose a signal into distinct frequency components, thereby enabling the extraction of valuable information. The application of a wavelet transform algorithm to motor encoder data facilitates a more precise analysis of the encoder's state and performance. In comparison to conventional methodologies, this technique enables the prompt identification of encoder faults and potential problems, thereby facilitating the implementation of timely maintenance and repairs.

2. Methodologies

To guarantee the seamless ingress and egress of passengers from train cars, it is imperative to create a hardware testing environment that can be practically implemented. The minimum width of the train doors must be 600 mm. However, considering exceptional emergency scenarios and to optimize the boarding and alighting process, the minimum width when the doors are open should be at least 800 mm. Consequently, the testing environment has been configured with the requisite widths, as illustrated in Fig. 2.

In establishing the wavelet transform simulation environment, in this study, we utilized the MATLAB simulator to obtain simulation curves under diverse conditions, including regular operation and encoder disconnection scenarios. The objective was to ascertain whether the wavelet transform functionality and simulation curves in the simulated environment were in

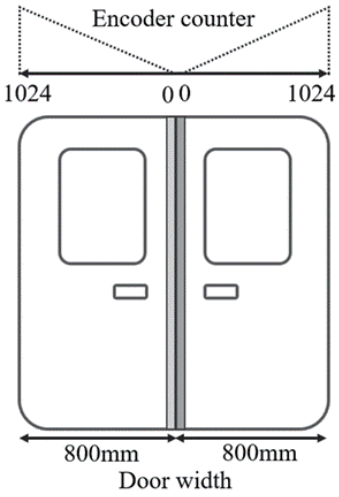

Fig. 2. Scale of the experimental platform utilized for the simulation of door mechanisms.

accordance with the original design requirements. The configuration of the simulation environment is illustrated in Fig. 3.

The initial step involved the utilization of a preprocessing module, which was employed to generate signals derived from the motor encoder. Subsequently, signal variations corresponding to different abnormal conditions were produced. Finally, the wavelet transform module was used to obtain distinguishable results by calculating the signals. This configuration effectively simulates a range of potential abnormal conditions, thereby facilitating the generation of reliable data for fault detection.

The encoder signal is an electrical voltage signal that is typically subjected to filtering and then converted through the use of dedicated hardware circuits. When the motor is operating in a steady state, the number of pulses per unit of time is constant in the context of the ideal theory. Consequently, the number of pulses and the time can be calculated to obtain a stable speed signal. By comparing the computed speed signal with the time, we can reasonably assess the speed within a given time unit, thereby determining the current state of the encoder.

The resolution of the encoder is defined as the number of pulses generated per revolution of the motor. Therefore, the angle for one revolution of the motor is 360° divided by the number of pulses generated per revolution, *P*. The number of pulses generated per second can be derived by considering the time unit as seconds. This data can be further converted into speed, expressed in revolutions per second (*RPS*) or revolutions per minute (*RPM*), as illustrated in Eq. (1).

$$RPS = N \div P,\ RPM = RPS \times 60\ (\text{s}) \tag{1}$$

In accordance with the aforementioned methodology, the speed signal is subject to processing via the implementation of a wavelet transform, thereby facilitating the subsequent analysis.

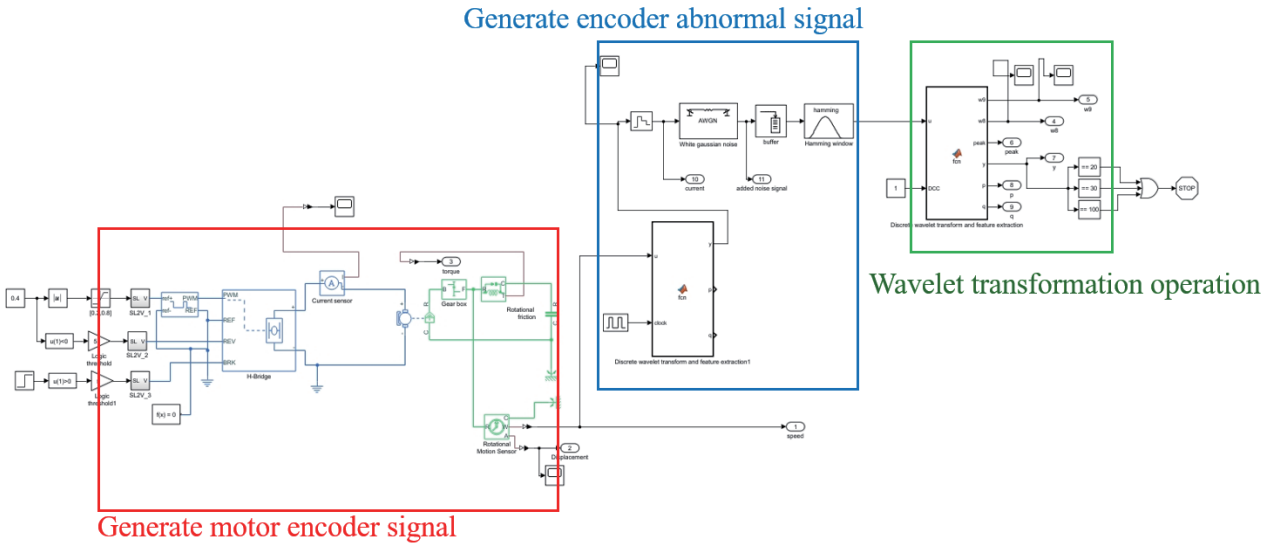

Fig. 3. (Color online) MATLAB simulation of motor encoder output and wavelet transform experiment.

Wavelet transform analysis offers numerous advantages. Its multiscale characteristics enable the observation of the original signal at varying degrees of detail, from coarse to fine. Additionally, the wavelet function of the band-pass filter can be regarded as a signal at different scales undergoing filtering. Furthermore, selecting an appropriate wavelet enables the wavelet transform to effectively characterize the local features of a signal in both the time and frequency domains. This facilitates the detection of the signal's exceptional components and transient states.

A smaller wavelet transform scale allows for comparing the wavelet function with a very small local signal, thereby obtaining a detailed signal with high-frequency characteristics. In contrast, a larger scale allows for a more extended analysis of the wavelet function along the time axis and a longer interval for signal analysis. This approach is primarily used to obtain the approximate contour state of the overall signal, which is extracted according to the low-frequency characteristics of the signals. In this study, the wavelet transform is employed to convert the speed signal of the encoder to detect anomalous signals. It is essential to obtain details of the low-frequency portion of the overall signal, which undergoes gradual changes, to accentuate the anomalous speed signal, thereby enabling the controller to detect encoder faults with greater expediency.

The DWT processes are illustrated in Fig. 4. The discrete input signal $X(n)$ is shown in the figure. The low-pass and high-pass filters, $g(k)$ and $h(k)$, are used to remove the high- and low-frequency components of the signal, respectively. The output signals $A_{1,L}(n)$ and $D_{1,H}(n)$ represent the approximation space and detail space converted from the original signal, respectively. A down-sampling filter, designated as $\downarrow Q$, is employed to reduce the sampling rate of a signal. Q is always 2, which represents the output signal $A_{1,L}(n)$ or $D_{1,H}(n)$ that is sampled at a rate of half that of the previous high-pass or low-pass filter output, effectively halving the sampling rate.

As illustrated in Eqs. (2) and (3) of the multiscale wavelet transform analysis, the signal can be decomposed into the approximation space and detail space through the filters in the wavelet function by multilevel analysis. The aforementioned equations illustrate the application of the a-scale wavelet transform in calculating the low- and high-frequency components of the signal at varying levels. The low- and high-frequency output components at level a are represented by $A_{a,L}(n)$ and $D_{a,H}(n)$, respectively. The previously described components are obtained by

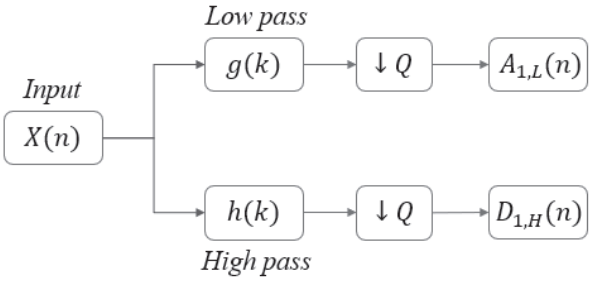

Fig. 4. Defined relationships and processes in DWT.

weighting the low-frequency signal from the preceding level ($a-1$), designated as $A_{a-1,L}(2n-k)$, with the filters $g(k)$ and $h(k)$. The filters thus determine how the signal from level $a-1$ is transformed into the low- and high-frequency components at level a. The multiscale wavelet transform describes a signal processing procedure used to decompose and analyze the low- and high-frequency components of the signal at a deep level.[18]

$$A_{a,L}(n)=\sum_{k=0}^{K-1}\mathrm{A}_{a-1,L}(2n-k)g(k) \tag{2}$$

$$D_{a,H}(n)=\sum_{k=0}^{K-1}A_{a-1,L}(2n-k)h(k) \tag{3}$$

Here, $g(k)$ and $h(k)$ represent the low- and high-pass filters, respectively, which are employed to extract the low- and high-frequency components of the signal. $A_{a,L}(n)$ represents the approximation space, which encompasses the low-frequency components obtained following the implementation of wavelet decomposition. $D_{a,H}(n)$ represents the detail space, which is used to describe the high-frequency components of the signal. The index "n" denotes the decomposed spaces, indicating the position of each detail or approximation space on the time axis. In this context, the variable "k" represents the filter index, which ranges from 0 to $K-1$, with K denoting the length of the filter. Moreover, the $(2n-k)$ coefficient denotes the index of the approximation signal space derived from the output of the preceding level.

Figure 5 demonstrates the DWT with a hierarchical structure of the multiscale wavelet transform. The multiscale wavelet transform is derived from the one-scale wavelet transform. Equations (4) and (5) elucidate the high- and low-pass transformations of a single scale. After the initial level of transformation, the resulting low-pass component is subjected to the transformations delineated in Eqs. (6) and (7), which constitute a two-scale transformation. The continuous α-scale wavelet transform is then employed, as illustrated in Eqs. (2) and (3). This process is continued until the step wave signal is rendered smooth.

$$A_{1,L}(n)=\sum_{k=0}^{K-1}X(2n-k)g(k) \tag{4}$$

$$D_{1,H}(n)=\sum_{k=0}^{K-1}X(2n-k)h(k) \tag{5}$$

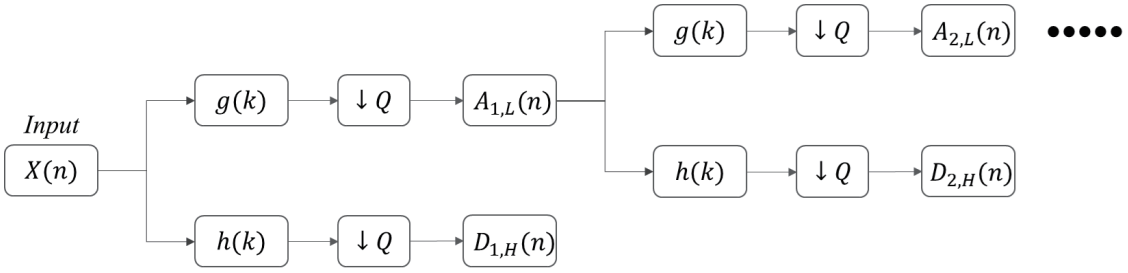

Fig. 5. Hierarchical structure of multiscale DWT.

Here, $X(n)$ represents a discrete input signal of length N, where N represents the total number of samples in the signal, and n takes values from 0 to $(N-1)$. In signal processing, the convolutional operation of the $(2n-k)$ index position of the input signal X with the index position k of the low-pass filtering function $g(k)$ is represented as $X(2n-k)g(k)$. The relative $X(2n-k)h(k)$ equation is used for the convolution operation of the high-pass filter.

The second-level wavelet transform is illustrated in the following equations:

$$A_{2,L}(n) = \sum_{k=0}^{K-1} A_{1,L}(2n-k)\, g(k), \tag{6}$$

$$A_{2,H}(n) = \sum_{k=0}^{k-1} A_{1,L}(2n-k)\, h(k). \tag{7}$$

The encoder of the door motor serves as an encoding device, converting the motor speed into a continuous-step wave signal. The long-term vibration during train driving and door opening and closing causes damage to the encoder and the connecting wires, resulting in loosened connections and poor contact. This leads to an error in the speed control of the door motor. Therefore, it is crucial to monitor the signal from the encoder to ensure its functionality. However, the motor running speed is not entirely fixed since the door motor operates during opening and closing. For example, during the initial phase of closure, the door's velocity is relatively lower, resulting in a longer duration of the encoder's step wave signal. As the door approaches the lock, the encoder's output signal transitions to a step wave of a shorter period, resulting in a motor speed signal that is a composite of high- and low-frequency signals. This composite signal is analogous to noise and is, therefore, challenging to analyze. Accordingly, in this paper, we propose a multiscale wavelet transform method to convert the encoder's motor speed signal into a smooth and stable waveform through a multilevel wavelet transform and amplify the features, which facilitates the quick and accurate detection of encoder issues.

By employing the fundamental definitions and calculations previously outlined, we can mitigate the noise present in the motor velocity encoder's continuous signal. This is accomplished by implementing a low-pass filter to eliminate high-frequency components through a series wavelet transform, producing a more readily comparable signal.

As illustrated in Fig. 6, the simulation was conducted under conditions where the encoder exhibited normal functionality. The speed presented in the simulated curve increased from zero to a constant, and it was determined that no faults occurred. The simulator presented a fault-free speed curve. This process enabled us to verify the system's performance under normal operating conditions and to obtain baseline data for comparison with abnormal situations. Subsequently, a series wavelet transform was applied to convert the simulated speed curve, generating a well-featured speed curve, as illustrated in Fig. 7. The results demonstrate that no encoder fault characteristics were identified.

Subsequently, a scenario in which the encoder signal is absent for one second will be presented. The MATLAB encoder fault signal simulation block was employed to generate the state where the encoder signal is lost. The resulting data waveform is illustrated in Fig. 8. The

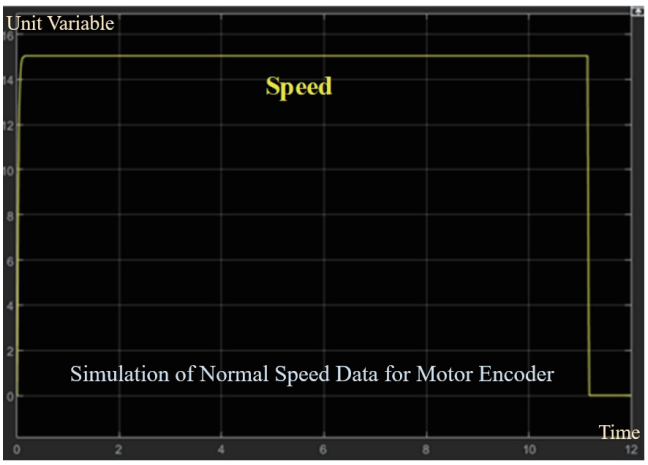

Fig. 6. (Color online) MATLAB simulation of motor encoder normal speed data.

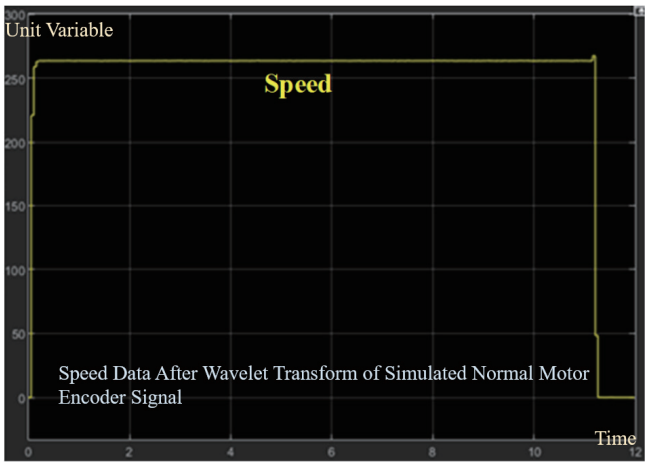

Fig. 7. (Color online) Speed data after wavelet transform of normal speed data.

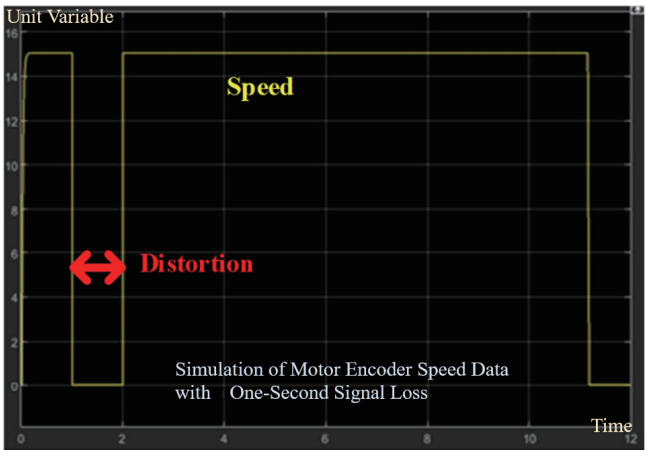

Fig. 8. (Color online) MATLAB simulation of motor encoder speed data with one-second signal loss.

waveform of the encoder signal with a one-second loss was then subjected to a series of wavelet transform computations. The output shown in Fig. 9 demonstrates that the abnormal features of the encoder fault signal are amplified. This illustrates the efficacy of the wavelet transform in highlighting the abnormal features.

As illustrated in Fig. 10, a 10% noise simulation test was conducted in an experiment with poor contact due to encoder wiring connection issues. One second after the commencement of the test, a 10% encoder noise signal was introduced, resulting in an irregularity in the speed curve. The MATLAB program was used to read the simulated curve of the abnormal case, which exhibited a 10% encoder noise signal introduced after 1 s. The waveform was subjected to a series of wavelet transforms and computations, as illustrated in Fig. 11. It can be observed that the anomalous features are amplified, thereby facilitating their analysis.

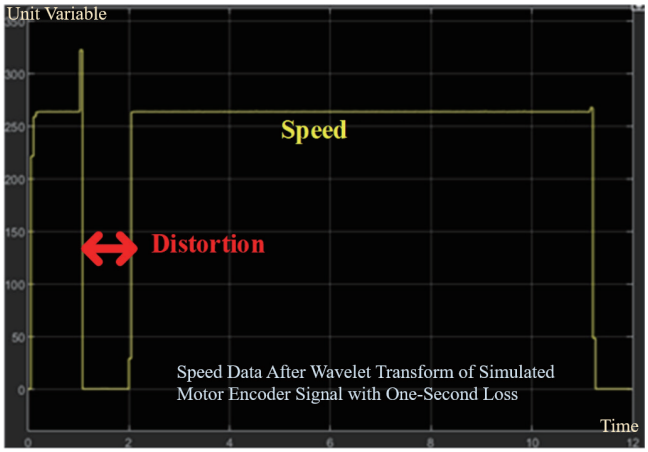

Fig. 9. (Color online) Speed data with one-second signal loss after wavelet transform.

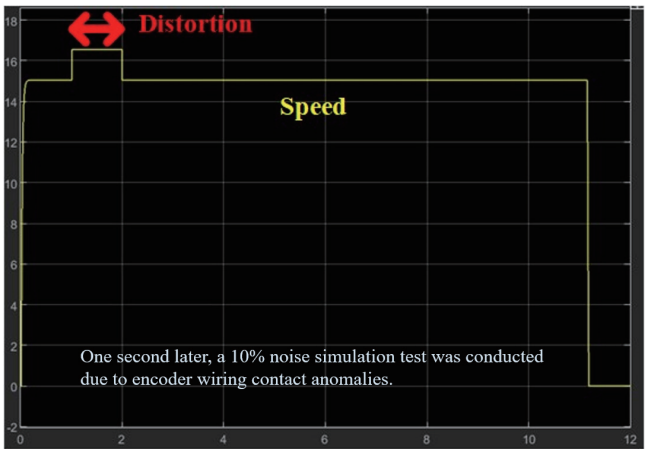

Fig. 10. (Color online) MATLAB simulates the speed data of a motor encoder, incorporating a wiring contact anomaly that occurs after a one-second interval.

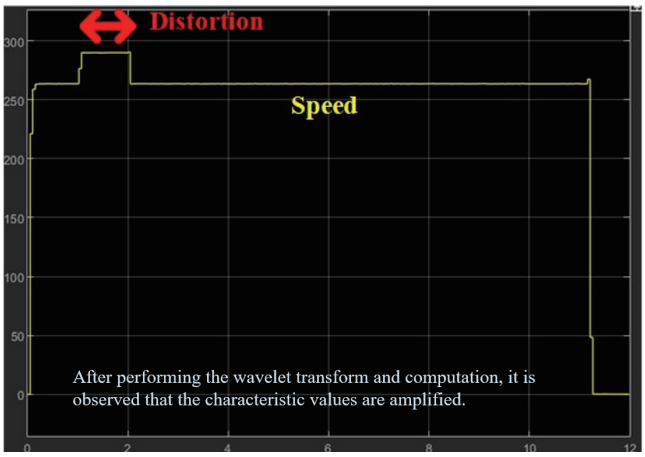

Fig. 11. (Color online) The speed data of wiring contact anomalies, following the application of a wavelet transform, are represented by a speed curve.

In the final experiment, as illustrated in Fig. 12, a door simulation mechanism is employed in conjunction with a motor and control driver to simulate the opening and closing of a train door. This simulation platform offers a highly realistic emulation of actual door movement, providing an experimental environment that closely resembles real-world conditions.

The motor and driver are indispensable elements for attaining the desired door motion and regulating the current and speed, thereby facilitating the opening and closing of the door. The microcontroller unit (MCU) serves as the central component of the control system and is responsible for receiving and processing data from the encoder. Subsequently, the extracted encoder signals are fed into a computer for data collection and processing. Subsequently, the wavelet transform results are subjected to analysis to ascertain whether the transformation is effective in amplifying the characteristic values.

This configuration provides a realistic and controllable experimental environment, facilitating the verification of the efficacy of the wavelet transform in amplifying anomalous features in encoder signals. In addition, implementing a genuine operational context can facilitate the secure operation of railway trains.

3. Results

As illustrated in Fig. 13, the motor encoder of the door simulation mechanism displays typical raw speed data, with the speed curve exhibiting a conventional trend. This indicates that during the test, the encoder operated normally without any faults or abnormalities. The resulting waveform after applying a series wavelet transform to the aforementioned speed data is shown in Fig. 14. It can be observed that the encoder speed curve exhibits no abnormalities. This indicates that in this experimental case, the output data from the encoder demonstrates stable and continuous characteristics without any apparent abnormalities or faults.

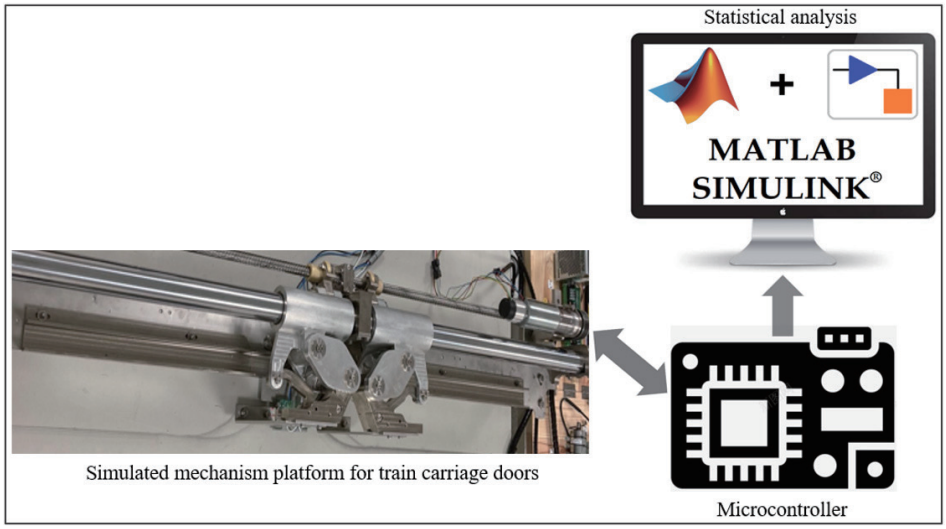

Fig. 12. (Color online) Experimental platform with door simulation mechanism and motor encoder.

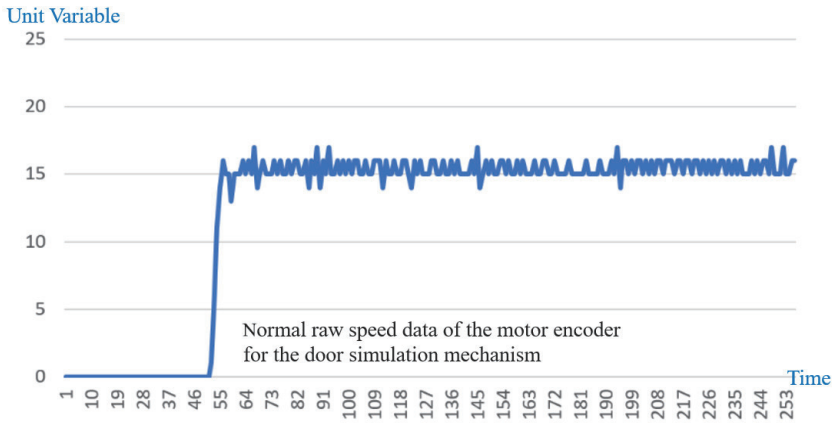

Fig. 13. (Color online) The MCU acquires the normal raw speed data from the motor encoder.

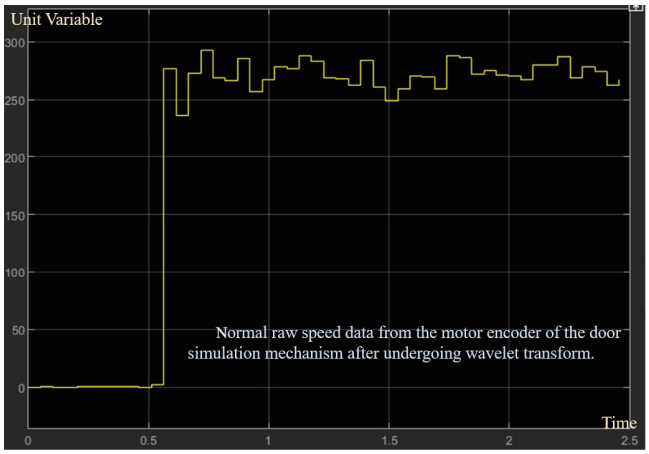

Fig. 14. (Color online) The normal raw speed data undergoes wavelet transformation.

As illustrated in Fig. 15, the raw speed data from the encoder of the door simulation mechanism displays a 1 s signal loss, whereby the speed data experiences a sudden interruption for approximately 1 s. This testing method is designed to simulate a scenario in which the motor encoder encounters a fault or is unexpectedly removed during operation, resulting in a failure in speed measurement. The resulting waveform after applying a series wavelet transform to the raw speed data, which includes a 1 s signal loss, is depicted in Fig. 16. It can be observed that the encoder signal is in an abnormal state while simultaneously amplifying its characteristic values indicative of the anomaly.

Figure. 17 illustrates the velocity data of the encoder with wiring contact issues in a door simulation mechanism. The speed data indicates the presence of a transient signal anomaly during the closing phase. This testing method is designed to simulate contact anomalies that may occur in the motor encoder during the door-closing process. The resulting waveform of the speed data from the encoder, following the application of a wavelet transform, is illustrated in Fig. 18.

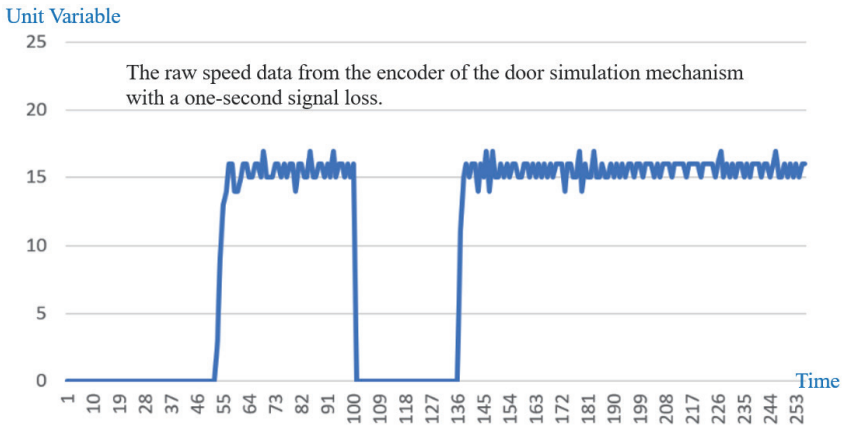

Fig. 15. (Color online) The MCU acquires the raw speed data from the motor encoder with a one-second signal loss.

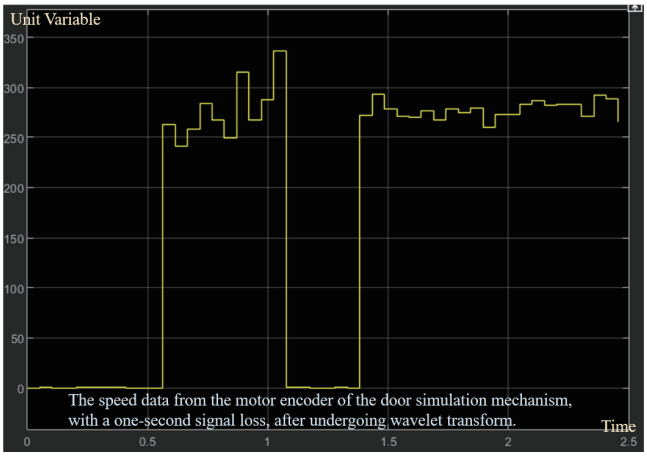

Fig. 16. (Color online) The raw speed data with a one-second signal loss undergoes wavelet transformation.

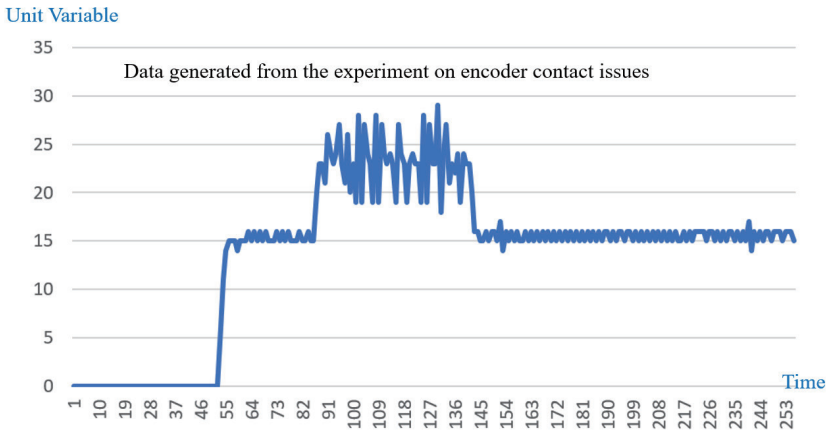

Fig. 17. (Color online) The MCU obtains speed data affected by poor encoder contact from the motor encoder.

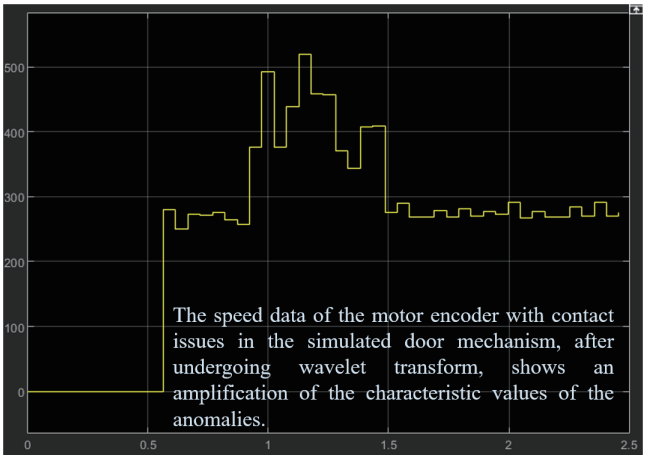

Fig. 18. (Color online) The raw speed data from the encoder with contact issues is processed through a wavelet transform.

The method demonstrates the existence of irregularities in the encoder signal and accentuates the distinctive values associated with these anomalies. This methodology allows for the accurate detection of encoder problems, thus enabling the implementation of timely adjustments and repairs to the system.

4. Conclusions

In this paper, we proposed a multiscale wavelet transform to convert the multifrequency chaotic curve of the speed signal of the motor encoder into a more stable speed curve while simultaneously highlighting and enhancing the features of the curve associated with abnormal conditions. This allows for the more straightforward detection of encoder faults. Firstly, in this study, we employed a simulation environment to simulate typical encoder signals and common

encoder issues, including malfunctions and poor wire connections. To this end, a wavelet transform is utilized to transform the simulated encoder speed signal into a more stable and readily analyzable signal curve, thereby validating the designed method. To demonstrate the applicability of the proposed method to a practical door device, we employed an experimental door and integrated the motor mechanism and MCU control driver to obtain the encoder's speed data. Subsequently, a series of wavelet transforms were performed to convert the signals. The results of the experiments demonstrated that the converted speed waveforms effectively amplify the characteristics of the abnormal encoder signals, which is beneficial for accurate detection. This approach facilitates the early detection of encoder failure and enables timely repair, thereby enhancing the reliability and stability of the system.

Acknowledgments

This work was supported by the Railway System Division, Mechanical and Mechatronics Systems Research Labs, Industrial Technology Research Institute Program 2023, Taiwan.

References

1 Z. Wang and L. Liu: Proc. 2019 IEEE 3rd Information Technology, Networking, Electronic and Automation Control Conf. (IEEE, 2019) 1989–1992. https://doi.org/10.1109/ITNEC.2019.8729537
2 W. Zhifei: Proc. 2019 12th Int. Symp. Computational Intelligence and Design Conf. (ISCID, 2019) 136–139. https://doi.org/10.1109/ISCID.2019.10114
3 L. Min, C. Zhaoyong, and Z. Jin: Proc. 2012 3rd Int. Conf. System Science, Engineering Design and Manufacturing Informatization (ICSSEM, 2012) 154–159. https://doi.org/10.1109/ICSSEM.2012.6340789
4 M. N. Saadi, M. Boukhenaf, A. Redjati, and N. Guersi: Proc. 2017 European Conf. Electrical Engineering and Computer Science (EECS, 2017) 101–106. https://doi.org/10.1109/EECS.2017.28
5 B. Noureddine, P. Remus, R. Raphael, and S. Salim: Proc. 2020 The 46th Annual Conf. IEEE Industrial Electronics Society (IEEE, 2020) 1088–1095. https://doi.org/10.1109/IECON43393.2020.9254401
6 J. Burriel-Valencia, A. Sapena-Baño, M. Pineda-Sanchez, and J. Martinez-Roman: Proc. 2015 IEEE Int. Conf. Industrial Technology. (IEEE, 2015) 775–780. https://doi.org/10.1109/ICIT.2015.7125192
7 J. Shim, G. C. Lim, and J. Ha: Proc. 2022 IEEE Applied Power Electronics Conf. and Exposition (IEEE, 2022) 1703–1708. https://doi.org/10.1109/APEC43599.2022.9773565
8 H. Liu and Y. Zhong: Proc. 2021 3rd Int. Academic Exchange Conf. Science and Technology Innovation (IAECST, 2021) 467–470. https://doi.org/10.1109/IAECST54258.2021.9695726
9 G. Avalos, S. Aguayo, J. Rangel-Magdaleno, and M. R. A. Paternina: Proc. 2022 Int. Conf. Electrical Machines (ICEM, 2022) 1830–1835. https://doi.org/10.1109/ICEM51905.2022.9910779
10 M. Fu, D. Du, F. Leng, J. Tian, Y. Fang, and J. Zhang: Proc. 2023 IEEE 6th Student Conf. Electric Machines and Systems (IEEE, 2023) 1–6. https://doi.org/10.1109/SCEMS60579.2023.10379246
11 N. Q. Hu, L. R. Xia, F. S. Gu, and G. J. Qin: IEEE Trans. Instrum. Meas. **60** (2011) 480. https://doi.org/10.1109/TIM.2010.2050980
12 N. P. Sakhalkar and P. Korde: Proc. 2017 Int. Conf. Energy, Communication, Data Analytics and Soft Computing (ICECDS, 2017) 363–367. https://doi.org/10.1109/ICECDS.2017.8390117
13 T. Yang, H. Pen, Z. Wang, and C. S. Chang: IEEE Trans. Instrum. Meas. **65** (2016) 549. https://doi.org/10.1109/TIM.2015.2498978
14 O. Zandi and J. Poshtan: Proc. 2018 Iranian Conf. on Electrical Engineering (ICEE, 2018) 827–833. https://doi.org/10.1109/ICEE.2018.8472458
15 I. Aydin and S. Seker: Proc. 2023 14th Int. Conf. Electrical and Electronics Engineering (ELECO, 2023) 1–5. https://doi.org/10.1109/ELECO60389.2023.10416018
16 R. Kechida and A. Menacer: Proc. 2011 2nd Int. Conf. Electric Power and Energy Conversion Systems (EPECS, 2011) 1–5. https://doi.org/10.1109/EPECS.2011.6126825
17 W. Bentrah, N. Bessous, S. Sbaa, R. Pusca, and R. Romary: Proc. 2020 Int. Conf. Electrical Engineering (ICEE, 2020) 1–7. https://doi.org/10.1109/ICEE49691.2020.9249925
18 S. G. Mallat: IEEE Trans. Pattern Analysis and Machine Intelligence **11** (1989) 674. https://doi.org/10.1109/34.192463